ON BUBBLE-SIDE TRANSPORT LIMITATIONS IN CATALYTIC FLUID-BED REACTORS

Abdullah A. Shaikh* and Saud H. Batran
Chemical Engineering Department
King Fahd University of Petroleum & Minerals
Dhahran 31261, Saudi Arabia

Abstract

The effect of bubble-side, mass transport limitations on performance of the catalytic fluidized-bed reactor is investigated. The reactor model of Werther (1980) is extended by introducing such resistance in its original formulation in the form of a dimensionless *Biot* number. Correlations for the *Biot* number are proposed. The modified model is contrasted with the original model to assess the extent of such resistance. It is shown that fluid-bed reactor performance is affected especially in the case of Geldart type-B particles and at low NTUs.

Keywords: Fluid bed reactor; Werther model; mass transfer resistance

*Corresponding author; Email: aashaikh@kfupm.edu.sa

INTRODUCTION

Several mathematical models for the catalytic fluidized-bed reactor have been developed over the last decades. The different models have been discussed and reviewed in various references, see e.g., Yates (1983); Doraiswamy and Sharma (1984); Wen (1984); Grace (1984); and Werther and Hartge (2003).

We address ourselves here to the model developed by Werther (1978, 1980); which has shown good agreement when compared to experimental data. While the original model of Werther may lack the sophistication of some of the more recently published models, such as those of Grace et al. (1999) and Werther and Hartge (2004), we feel it remains a useful tool for preliminary design and scale-up of fluidized-bed reactors on the basis of several characteristics. It is free from adjustable parameters; influence of reactor diameter on bed hydrodynamics is accounted for; and influence of different types of solids and existence of maximum bubble diameter are recognized. Moreover, a set of empirical expressions is available to complement the model. Indeed, Pell (1990) has gone so far as to describe the model as "the best for commercial systems".

An implicit assumption in the original Werther model is the absence of concentration gradients within the bubble-phase, and hence the absence of bubble-side mass transport limitation. This assumption, however, may be justified in the case of reactant-rich feeds, and in case of relatively slow reactions. In practical situations, the reactant might be part of a mixture or diluted by inert species so that the assumption of negligible bubble-side mass transport resistance becomes debatable. Likewise, there are reactions that are very rapid, so that mass-transfer in the bubble side could be significant in determining reactor performance.

The purpose of this communication is to extend the original Werther model (henceforth called OWM) to cases involving significant bubble-side mass transport resistance, and to examine the influence of such resistance on catalytic fluid-bed reactor performance.

MODIFIED MATHEMATICAL MODEL

The resistance to mass transfer in the bubble-side is assumed to lie in a film of a thickness $?_g$, defined by the film theory as D/k_g, as shown in Figure 1; while the resistance in the emulsion-side occurs in another film $?$, as defined in the OWM. The reaction occurs in the film $?$ and rest of emulsion phase. The basic assumptions made in OWM are retained; namely, that the gas-phase is in plug flow and gas flow rate in the emulsion phase is negligible. Based on the above concepts and assumptions, the dimensionless material balance equations and associated initial and boundary conditions, for a first-order reaction, are given as follows:

Reactor Balance:

$$\frac{dX_A}{dL} = (Bi)(NTU)\left(1 - X_A\right)\left(1 - \overline{C}\big|_{Y=0}\right) \tag{1}$$

$$L = 0, \quad X_A = 0 \tag{1a}$$

Bubble-Emulsion Balance

$$\frac{d^2\overline{C}}{dY^2} = Ha^2\overline{C} \tag{2}$$

$$Y = 0, \quad \frac{d\overline{C}}{dY} = Bi(1 - \overline{C}) \tag{2a}$$

$$Y = 1, \quad \frac{d\overline{C}}{dY} = Ha^2\left(\frac{\beta}{\gamma}\right)\overline{C} \tag{2b}$$

Solving the above model equations yields a relationship for reactant conversion as follows:

$$X_A = 1 - \exp\left[\frac{\left(\frac{\left(\frac{Ha - \tanh(Ha)}{1 - \left(\frac{Ha}{Bi}\right)\left(\frac{Ha - \tanh(Ha)}{1 - \left(\frac{Ha}{Bi}\right)Ha\tanh(Ha)}\right)}\right)(Ha)NTU}{1 - \left(\frac{Ha}{Bi}\right)\left(\frac{Ha - \tanh(Ha)}{1 - \left(\frac{Ha}{Bi}\right)Ha\tanh(Ha)}\right)}\right)}{1 - \left(\frac{Ha}{Bi}\right)\left(\frac{Ha - \tanh(Ha)}{1 - \left(\frac{Ha}{Bi}\right)Ha\tanh(Ha)}\right)}\right] \quad (3)$$

Note that the parameters in eq. (3) are the same as the ones appearing in the OWM, except for the new parameter *Bi, Biot* number, which reflects the effect of transport resistance in the bubble-side. Here we define *Bi* by:

$$Bi = \frac{k_g}{k_c} \quad (4)$$

Note also that in the limit of a high value of *Bi*, eq. (3) reduces identically to the corresponding conversion relationship in the OWM. While Werther proposed correlations to evaluate k_c, there appears to be no expressions in the literature for k_g in fluidized-bed reactors. Therefore we propose to evaluate k_g by analogy with gas-liquid systems. The following relationship has been proposed for gas bubbles in liquids (Barona, 1979), which is rooted in the classic work of Newman:

$$k_g = 6.58\frac{D}{d_b}\frac{P}{p_i} \quad (5)$$

Therefore the parameter *Bi* can be evaluated by combining eq. (4), eq. (5) and the correlations presented by the Werther (1984) to predict the bubble-emulsion mass-transfer coefficient k_c. This yields the following correlations:

$$Bi = \begin{cases} 414\dfrac{D}{d_b}\dfrac{P}{p_i} & \text{group A powders} \\ 748\dfrac{D}{d_b}\dfrac{P}{p_i} & \text{group B powders} \end{cases} \quad (6)$$

It should be emphasized that eq. (5) is based on gas-liquid systems. Obviously bubbles in fluidized beds do not possess the same characteristics as those in gas-liquid

systems. However, eq. (6) may serve for preliminary assessment of bubble-side transport limitations

RESULTS AND ANALYSIS

Parametric Studies

In order to study the significance of bubble-side resistance, the influence of *Bi* on the *ratio* of the exit conversion in the presence of bubble-side resistance to that without bubble-side resistance was investigated at various values of Ha, ? , and NTU. Figure 2a shows the effect of *Ha* on the ratio of conversions at fixed values of ? and NTU, while the effects of ? and *NTU* are shown in Figures 2b and Figure 2c, respectively. It should be noted that the range of parameters in Figures 2a-2c is typical of that encountered in practice. In fact, the distinction between the behavior of the two groups of solids commonly used in industry, group A and group B, allows us to define an "active" area for each group, as shown in Figure 2c. This was achieved with the aid of the set of correlations for the OWM and the defined ranges in the Geldart chart in addition to the common operating conditions for bubbling fluidized-bed reactors (cf. Grace, 1986).

Hatta number is a measure of reactivity: the higher *Ha* is, the faster the reaction. It is obvious from Figure 2a that the effect of *Bi* is more pronounced when the reaction is fast. Note that the achievable conversion is within 40% of that without gas-side resistance when *Bi*=0.2 and *Ha* ? (0.1-1.0). The relative magnitudes of the reaction rate to the bubble-side mass transfer rate play an important role. When the reaction rate is slower, the bubble-side resistance is overshadowed by the kinetics and no transport limitations appear. On the other hand, when the reaction rate is faster, the effect of the bubble-side resistance appears and the reaction becomes limited, to some degree, by the transport in the gas-side.

The parameter ? is interpreted as the ratio of film volume to emulsion volume. Therefore the most important parameter that affects ? is the interfacial area *a*. The other parameters (in the definition of ?) change within limited ranges. Figure 2b shows that an increase in the value of ? increases the ratio of conversions. The parameter ? is larger when *a* is large, and this is a direct result from the smaller bubble diameters. The smaller bubble diameters have another effect: increase in the bubble-side mass-transfer coefficient k_g, as can be seen from eq. (5), and hence bubble-side mass-transfer resistance decreases. This explains why the conversions curves of the modified model and the OWM approach one another as ? increases.

The number of transfer units *NTU*, on the other hand, is a function of the operating conditions and scale of the reactor. A look at Figure 2c shows that the ratio of conversions decreases as *NTU* decreases. The reason is that a low value of *NTU* indicates that the gas residence time is short and/or mass transfer in the emulsion phase is poor. Consequently, the reaction is not able to compensate for the transport limitations in the bubble-side.

As alluded to earlier, the difference in the behavior of group-A and group-B powders allows us to draw general conclusions. It is apparent from Figure 2c that a fluidized-bed reactor with group-A powders is affected the least. This is attributed mainly to the smaller bubble size d_b. This leads to higher values of *Bi*, ? and *NTU*, thus reducing the effect of bubble-side mass transfer resistance.

Model Validation

The OWM has been used to fit experimental data for some first-order reactions, reported in the literature (Werther, 1980). We have in turn applied the modified model to fit two of the same reaction systems, namely, the catalytic decomposition of nitrous oxide (Massimilla and Johnstone, 1961), and the catalytic oxidation of ammonia (Shen and Johnstone, 1955). Hydrodynamic and reaction conditions for both systems are shown in Tables 1. Although both studies are fairly dated, they can be gainfully employed to verify our central hypothesis as both reaction systems are reactant lean.

As shown in Figures 3 and 4, some improvement is observed especially in the region where the gas velocity is not high, i.e. at low NTU values. The values of *Bi* are also plotted on the same figures. Note that *Bi* decreases with gas velocity as expected. We hasten to add that comparing the ability to fit experimental data by the two models does not necessarily reveal the importance of gas-side resistance, because some parameter values of the two models change by fitting.

CONCLUDING REMARKS

We have extended the original Werther model for catalytic fluid-bed reactors to cases involving appreciable bubble-side resistance to mass transfer. Our analysis was admittedly presented in terms of linear kinetics; however extension to other kinetics should not be mathematically or numerically intractable. Useful correlations for the *Biot* number have been developed, however we are cognizant that they are rooted in analogy with gas-liquid systems which bear superficial similarities to bubbles in fluidized beds.

We have found that bubble-side resistance is important in cases where the reactant is part of a mixture, or when the reaction is fast. Our analysis demonstrates that this resistance is important when the number of transfer units is low or when the fluidized powder belongs to Geldart's group B.

Nomenclature

a	specific bubble interfacial area [m^{-1}]
Bi	*Biot* number, defined by equations (4) and (6)
C	concentration of reactant A [mol m^{-3}]
$\bar{C}$	dimensionless concentration defined as C_{Ad}/C_{Ab}
d_b	equivalent bubble diameter [m]
D	average species diffusivity [m^2 s^{-1}]
h	height above distributor plate [m]
H	expanded bed height [m]
H_{mf}	bed height at minimum fluidization [m]
Ha	*Hatta* number, defined as $\sqrt{kD}/k_c$
k	reaction rate constant [s^{-1}]
k_c	bubble to emulsion mass transfer coefficient, [m s^{-1}]
k_g	gas-side mass transfer coefficient, [m s^{-1}]
L	dimensionless bed height, defined as h/H
NTU	number of transfer units, defined as $k_c aH/(u-u_{mf})$
P	total pressure [pa]
p_i	partial pressure of inert gas species [pa]
u	superficial gas velocity [m s^{-1}]
u_{mf}	minimum fluidization velocity [m s^{-1}]
X_A	reactant conversion, defined as $(1-C_{Ab}/C_{A0})$
y	distance inside emulsion phase [m]
Y	dimensionless distance inside emulsion phase, defined as y/d

Greek symbols

d	film thickness [m]
e	bubble gas hold-up
F	ratio of film volume to emulsion volume, defined as $aD/k_c(1-e_b)$

Subscripts

b	bubble phase
d	dense phase
g	bubble phase

References

Barona, N., 1979, Design CSTR reactors this way, Hydrocarbon Processing, 58(7): 179.

Doraiswamy, L.K. and Sharma, M.M., Heterogeneous Reactions: Analysis, Examples, and Reactor Design. Volume 1: Gas-Solid and Solid-Solid Reactions, Wiley, New York, 1984.

Grace, J.R., "Generalized models for isothermal fluidized bed reactors", in Recent Advances in Engineering Analysis of Chemically Reacting Systems, Doraiswamy, L.K. (ed.),Wiley Eastern, New Delhi, 1984.

Grace, J.R., "Fluid beds as chemical reactors", in Gas Fluidization Technology, Geldart, D. (ed.), Wiley, New York, 1986.

Grace, J.R., Abba, I.A., Hsiaotao, B., and Thompson, M.L., 1999, Fluidized bed catalytic reactor modeling across the flow regimes, Canadian Journal of Chemical Engineering, 77:305-311

Massimilla, L. and Johnstone, H.F., 1961, Reaction kinetics in fluidized beds, Chemical Engineering Science, 16: 105-112.

Pell, M., Gas Fluidization, Elsevier, Amsterdam, 1990.

Shen, C.Y. and Johnstone, H.F., 1955, Gas-solid contact in fluidized beds, AIChE Journal, 1(3): 349-365.

Wen, C.Y., "Flow regimes and flow modeling fluidized bed reactors", in Gas Fluidization Technology, Geldart, D. (ed.), Wiley, New York, 1986.

Werther, J., 1978, Scale-up of fluidized bed reactors, German Chemical Engineering, 1: 243.

Werther, J., 1980, Modeling and scale-up of industrial fluidized bed reactors, Chemical Engineering Science, 35: 372-379.

Werther, J., "Hydrodynamics and mass transfer between the bubble and emulsion phases in fluidized beds of sand and cracking catalyst", in Fluidization, D. Kunni and R. Toei (eds.) Engineering Foundation, New York, 1984

Werther, J. and Hartge, E.-U., 2003, Modeling of fluidized bed reactors, International Journal of Chemical Reaction Engineering, 1: 1-47.

Werther, J. and Hartge, E.-U., 2004, Modeling of industrial fluidized-bed reactors, Industrial and Engineering Chemistry Research, 43: 5593-5604.

Yates, J.G., 1983, Fundamentals of Fluidized-Bed Chemical Processes, Butterworth, London.

Table 1: Hydrodynamic and reaction data for simulation of NH_3 oxidation and N_2O decomposition

Parameter	**Catalytic NH_3 Oxidation**	**Catalytic N_2O decomposition**
Feed Composition	10 % NH_3; 90% O_2	1 % N_2O; 99% air
Temperature	523 K	672 K
Pressure	1.1 bar	1 bar
Bed diameter	0.114 m	0.114 m
H_{mf}	0.58 m	1.09 m
u	0.01 – 0.17 m s^{-1}	0.01 – 0.06 m s^{-1}
k (OWM)*	0.0446 s^{-1}	0.005 s^{-1}
k (this work)*	0.0493 s^{-1}	0.008 s^{-1}

***** fitted parameter

Captions for Figures

Figure 1 Concentration profiles within bubble and emulsion sides

Figure 2a Effect of Hatta and Biot numbers on the ratio of conversions

Figure 2b Effect of the parameter F and Biot number on the ratio of conversions

Figure 2c Effect of number of transfer units and Biot number on the ratio of conversions

Figure 3 Model comparisons with experimental results for catalytic oxidation of ammonia at 523 K and H_{mf}=0.58 m, data of Massimilla and Johnstone (1961)

Figure 4 Model comparisons with experimental results for catalytic decomposition of nitrous oxide at 672 K and H_{mf} =1.09 m, data of Shen and Johnstone (1955)

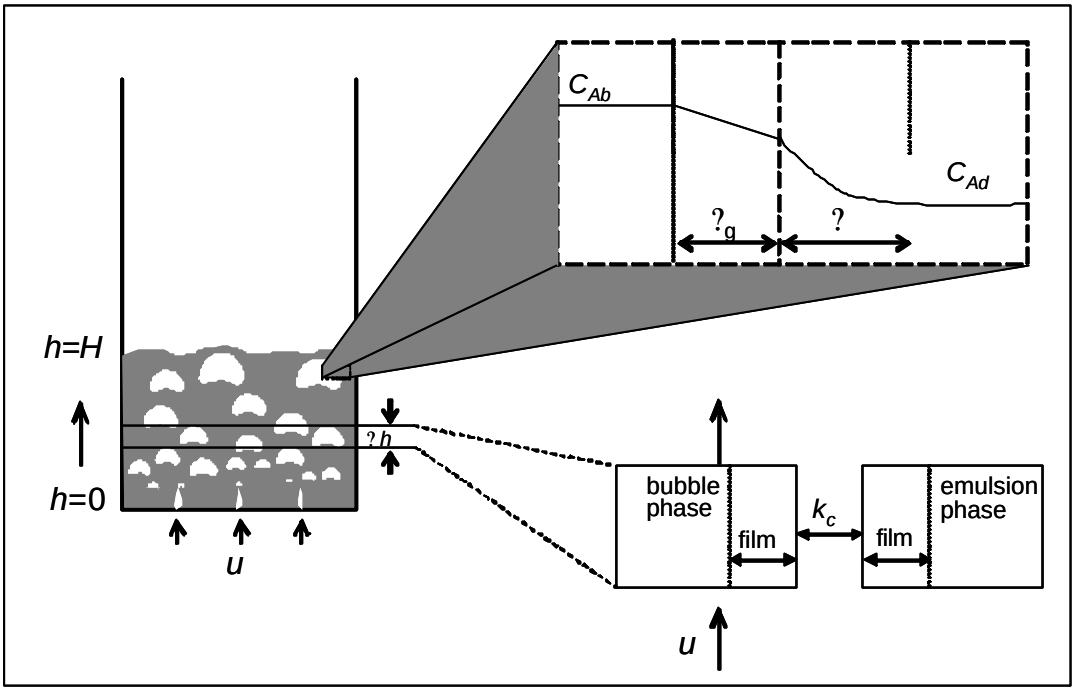

Figure 1

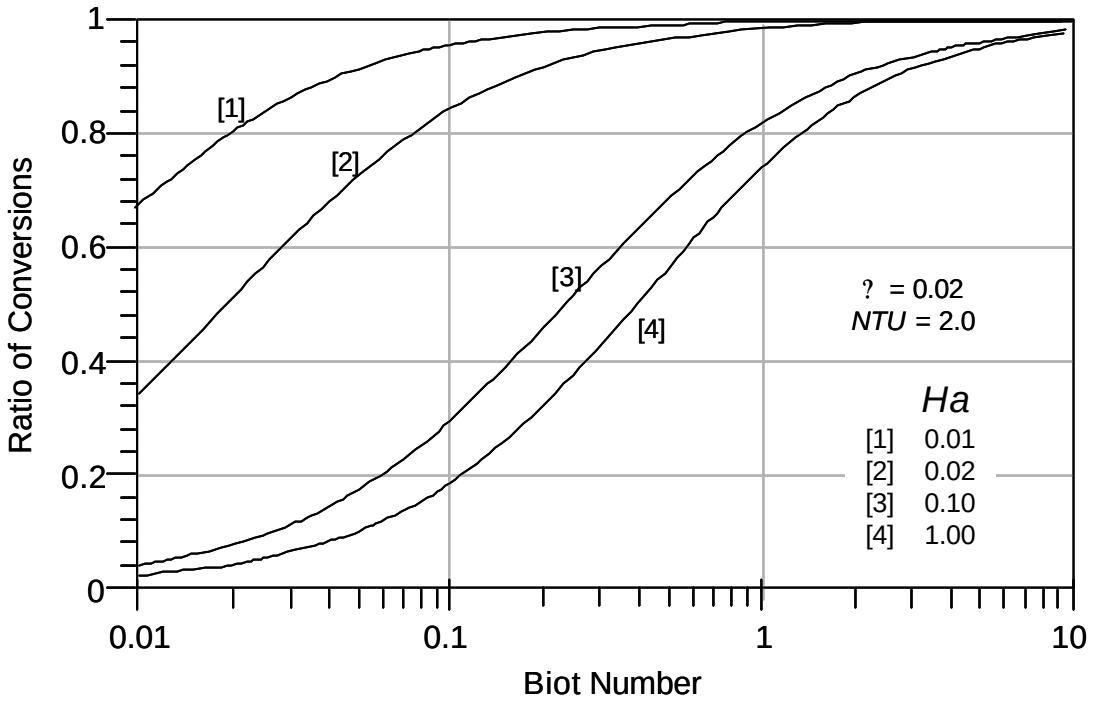
Ratio of Conversions
Biot Number
1
0.8
0.6
0.4
0.2
0
0.01
0.1
1
10
[1]
[2]
[3]
[4]
? = 0.02
NTU = 2.0
Ha
[1] 0.01
[2] 0.02
[3] 0.10
[4] 1.00

Figure 2a

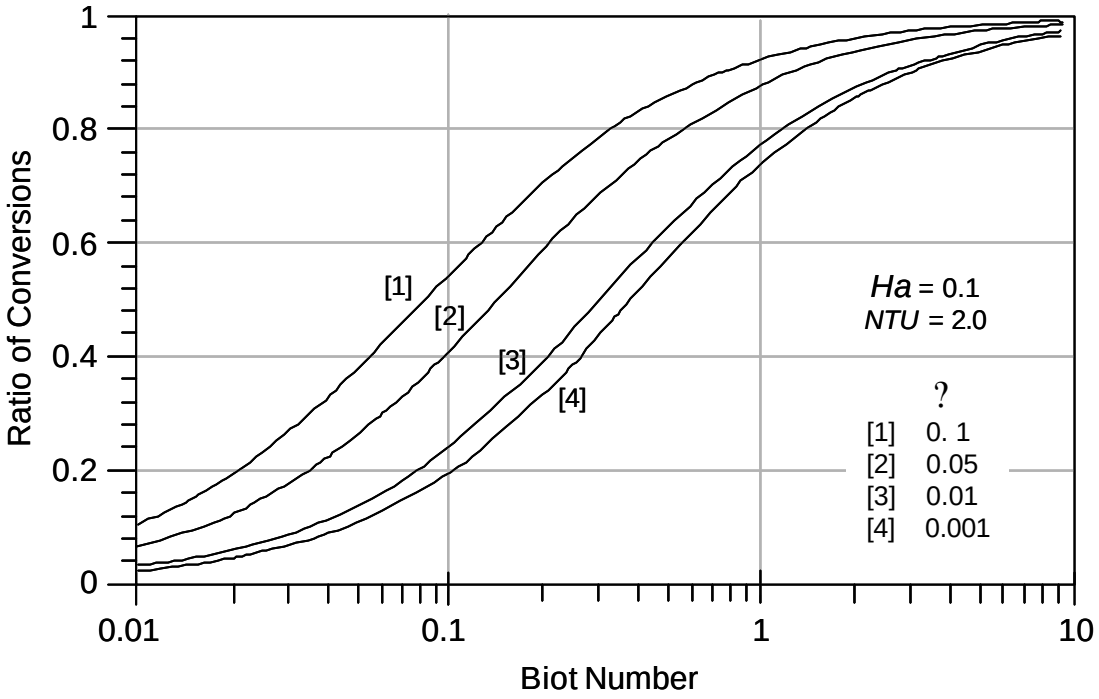
Ratio of Conversions
Biot Number
1
0.8
0.6
0.4
0.2
0
0.01
0.1
1
10
[1]
[2]
[3]
[4]
Ha = 0.1
NTU = 2.0
?
[1] 0. 1
[2] 0.05
[3] 0.01
[4] 0.001

Figure 2b

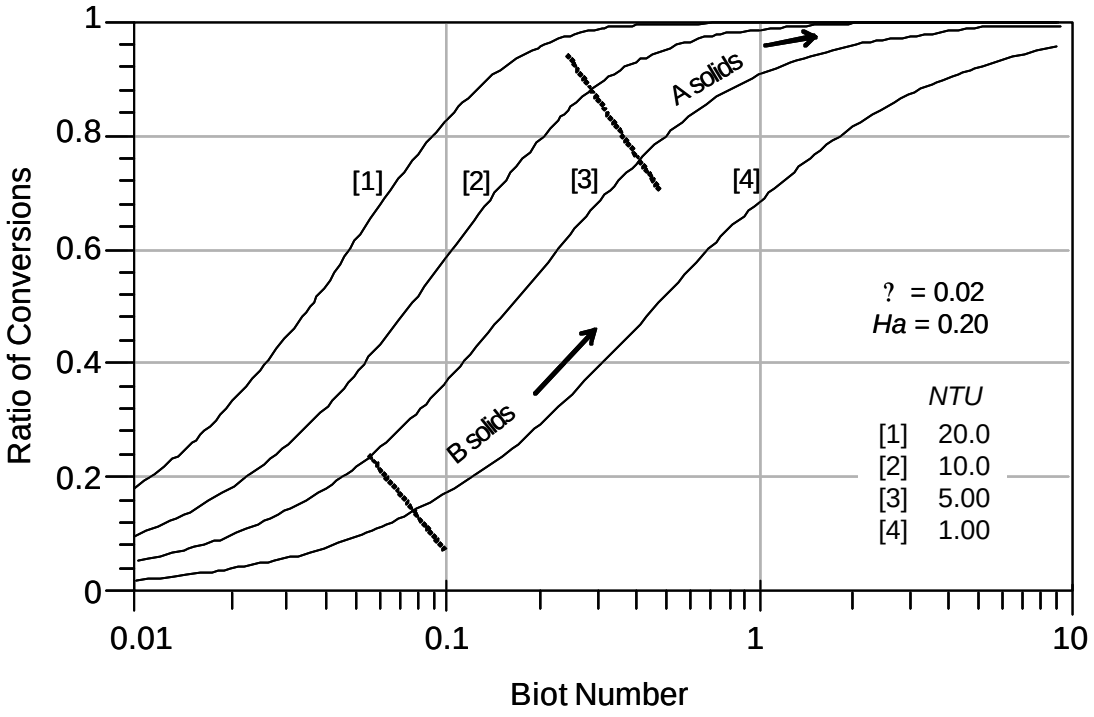
Ratio of Conversions
Biot Number
1
0.8
0.6
0.4
0.2
0
0.01
0.1
1
10
[1]
[2]
[3]
[4]
A solids
B solids
? = 0.02
Ha = 0.20
NTU
[1] 20.0
[2] 10.0
[3] 5.00
[4] 1.00

Figure 2c

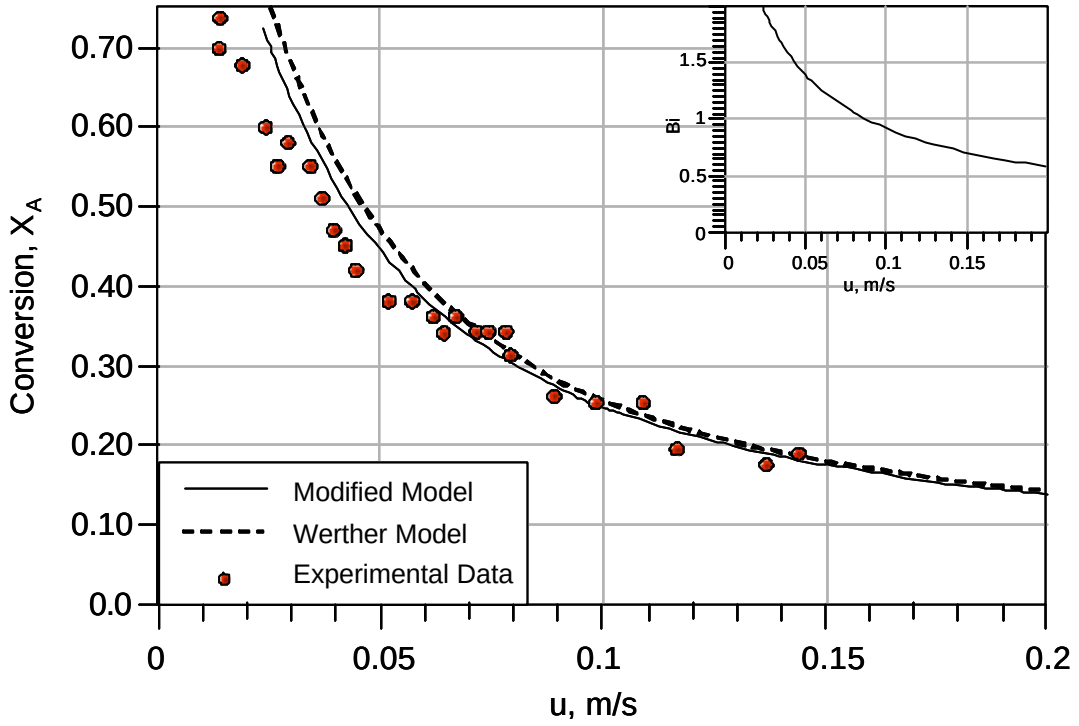
Conversion, X_A
0.70
0.60
0.50
0.40
0.30
0.20
0.10
0.0
0
0.05
0.1
0.15
0.2
u, m/s
Modified Model
Werther Model
Experimental Data
Bi
1.5
1
0.5
0
0
0.05
0.1
0.15
u, m/s

Figure 3

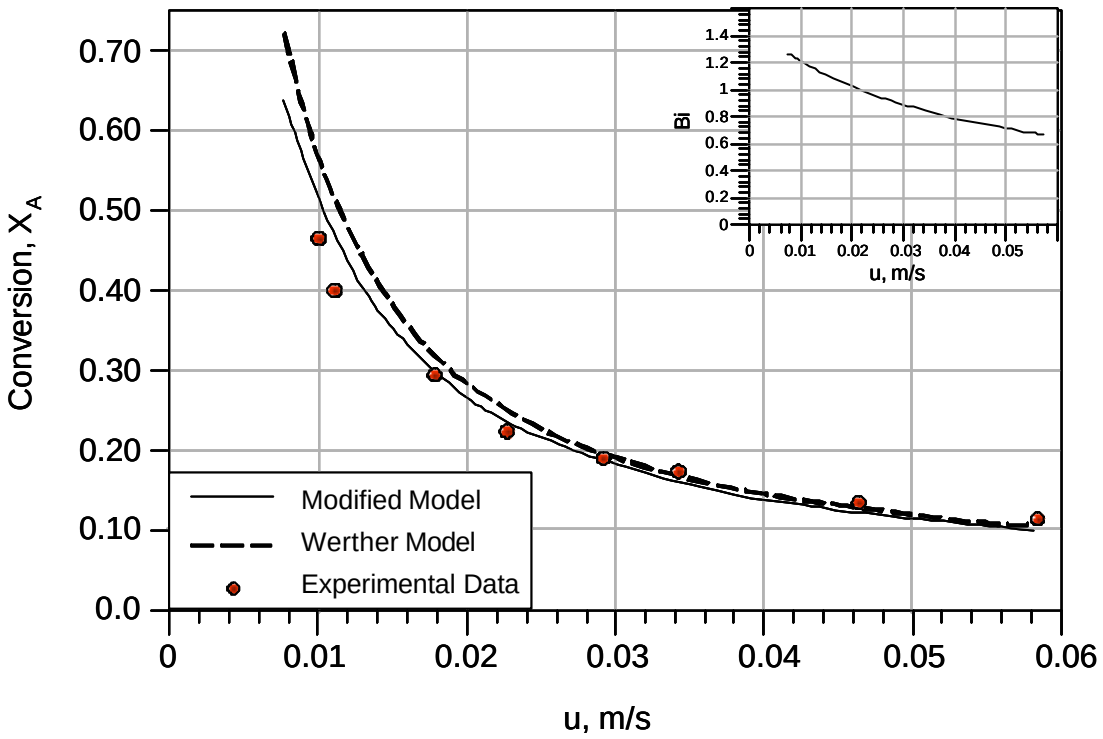
Conversion, X_A
0.70
0.60
0.50
0.40
0.30
0.20
0.10
0.0
0
0.01
0.02
0.03
0.04
0.05
0.06
u, m/s
Modified Model
Werther Model
Experimental Data
Bi
1.4
1.2
1
0.8
0.6
0.4
0.2
0
0
0.01
0.02
0.03
0.04
0.05
u, m/s

Figure 4